Electronic Supplementary Material (ESI) for Nanoscale.
This journal is © The Royal Society of Chemistry 2023

Supplementary Information

Ni/Co/Co_3O_4@C Nanorods Derived from MOF@MOF Hybrid for Efficient Overall Water Splitting

Dao Thi Dung,[a,b,†] Do Van Lam,[a,†] Euijin Roh,[c] Sanghyeon Ji[d], Jong Min Yuk[d], Jae-Hyun Kim,[a,b] Hyunuk Kim,[b,c] and Seung-Mo Lee[a,b,*]

[a] Korea Institute of Machinery and Materials (KIMM), 156 Gajeongbuk-ro, Yuseong-gu, Daejeon 34103, South Korea.

[b] University of Science and Technology (UST), 217 Gajeong-ro, Yuseong-gu, Daejeon 34113, South Korea.

[c] Korea Institute of Energy Research (KIER), 152 Gajeong-ro, Yuseong-gu, Daejeon 34129, South Korea.

[d] Korea Advanced Institute of Science and Technology (KAIST), 291 Deahak-ro, Yuseong-gu, Deajeon, 34141, South Korea.

[†] These authors contributed equally to this work.

* Corresponding author: Seung-Mo Lee (sm.lee@kimm.re.kr)

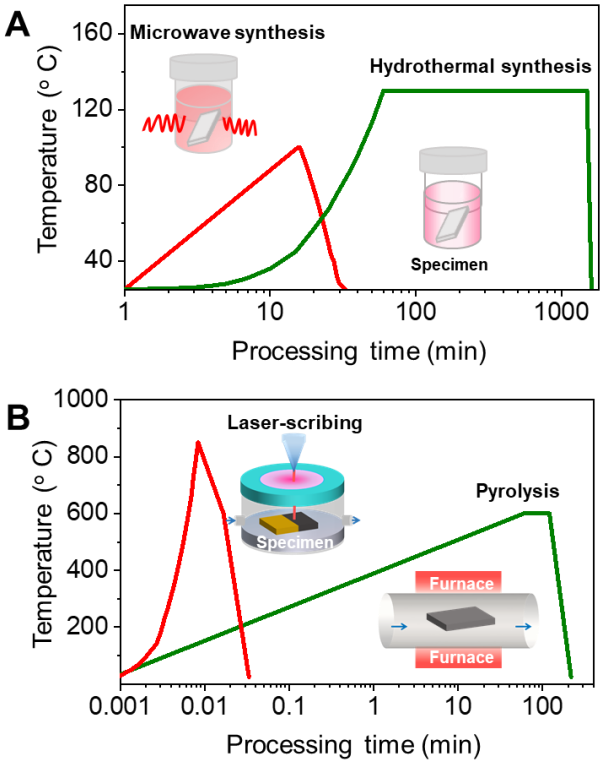

Figure S1. (A) The time-temperature profiles of the microwave and hydrothermal synthesis. The microwave synthesis of the Co/Ni-MOF nanorods on Ni foam was swiftly conducted for 2 min at 100 ºC, whereas the hydrothermal synthesis of Co/Ni-MOF lasted for 24 h at 130 ºC. (B) The time-temperature profiles of the laser-scribing and pyrolysis process. The pyrolysis took several hours in a furnace, whereas the laser-scribing took only a few seconds.

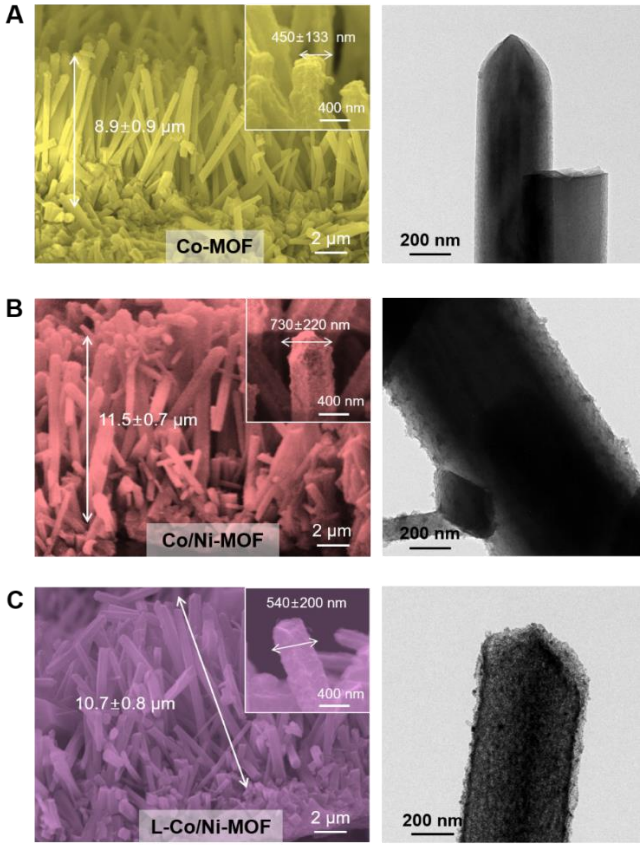

Figure S2. SEM and TEM images of (A) Co-MOF, (B) Co/Ni-MOF, and (C) L-Co/Ni-MOF.

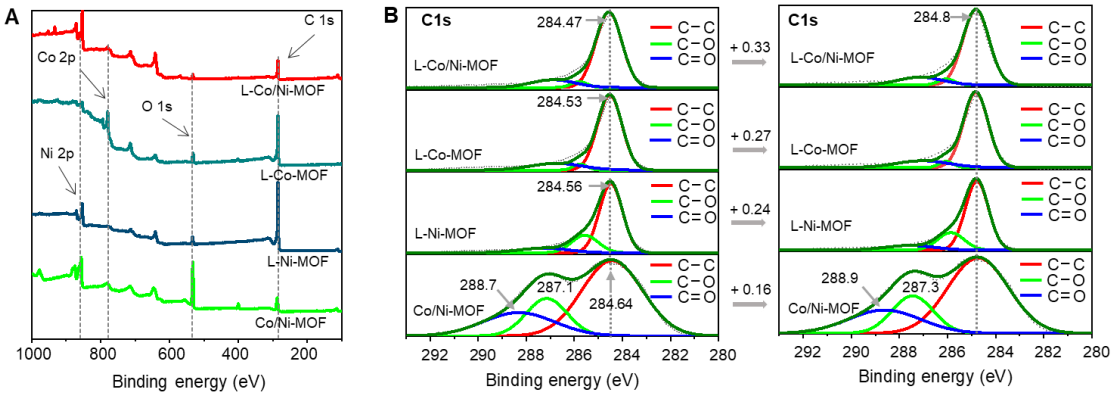

Figure S3. (A) XPS survey scan spectra of samples. (B) Deconvoluted C1s XPS spectra of samples before and after calibration. The C1s peak was used as a reference for the calibration, which was assumed to have a binding energy of 284.8 eV [S1, S2].

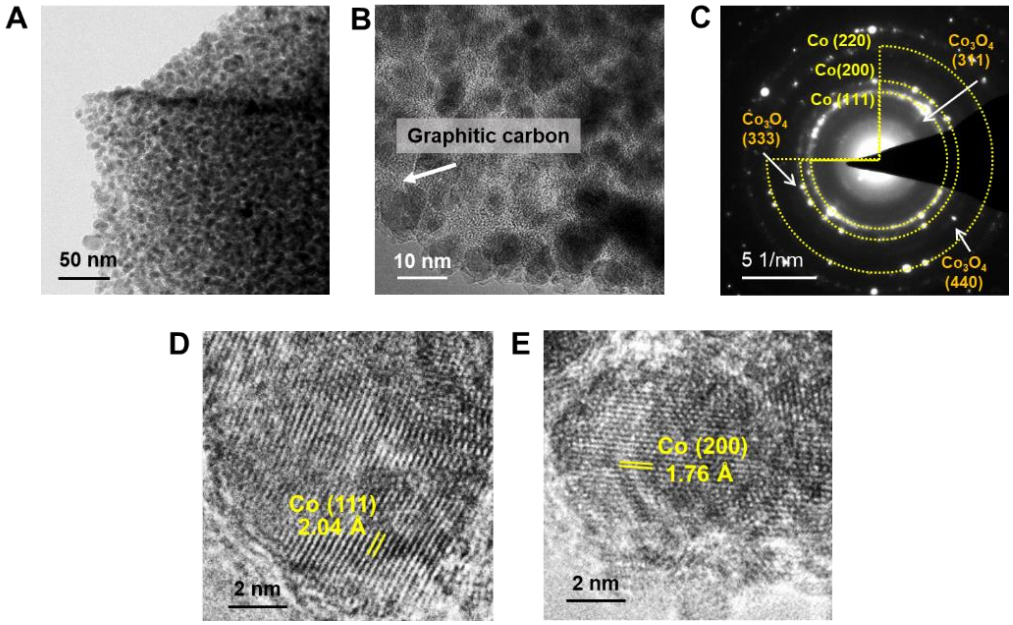

Figure S4. Phase and microstructure characteristics of the L-Co-MOF. (A, B) TEM images showing the microstructure of a representative L-Co-MOF nanorod. (C) SAED pattern. (D, E) HRTEM images showing the crystalline nanoparticles of Co with (111) and (200) planes.

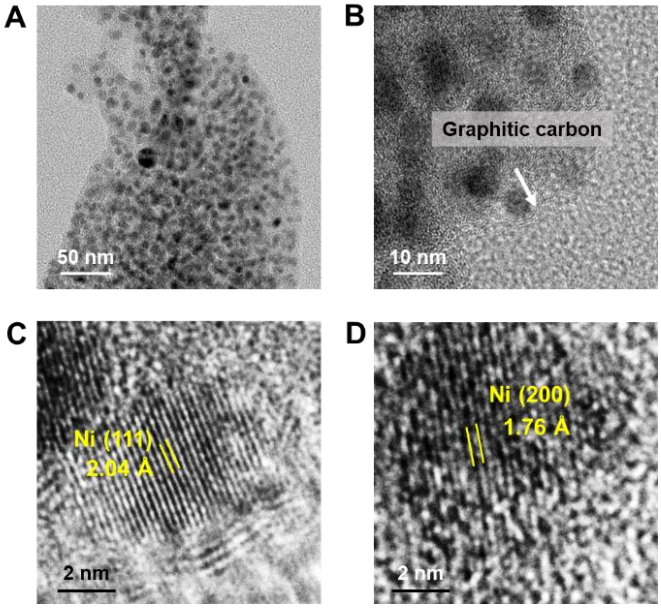

Figure S5. Phase and microstructure characteristics of the L-Ni-MOF. (A, B) TEM images showing the microstructure of a representative L-Ni-MOF nanorod. (C, D) HRTEM images showing the crystalline nanoparticles of Ni with (111) and (200) planes.

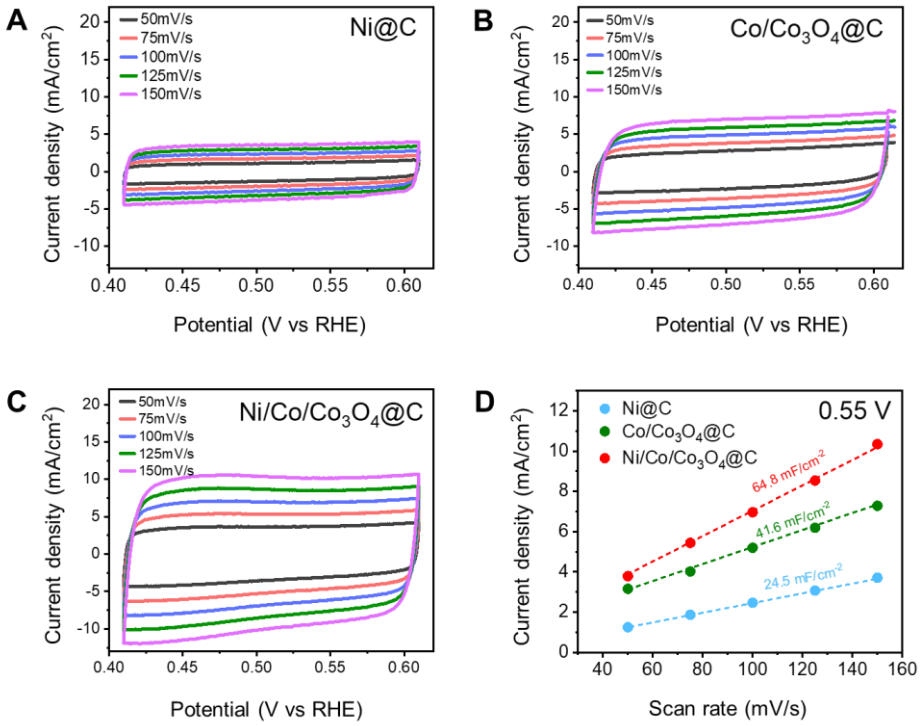

Figure S6. Cyclic voltammetry profiles of the samples at different scan rates in a non-Faradaic potential range of 0.41 - 0.61 V vs RHE. (A) Ni@C, (B) Co/Co_3O_4@C, and (C) $Ni/Co/Co_3O_4$@C. (D) A plot of current density vs scan rate at a potential of 0.55 V vs RHE.

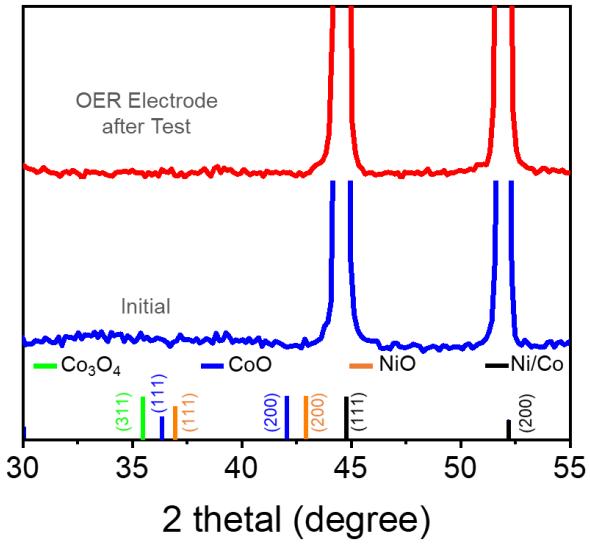

Figure S7. XRD patterns of the $Ni/Co/Co_3O_4$@C before and after the OER.

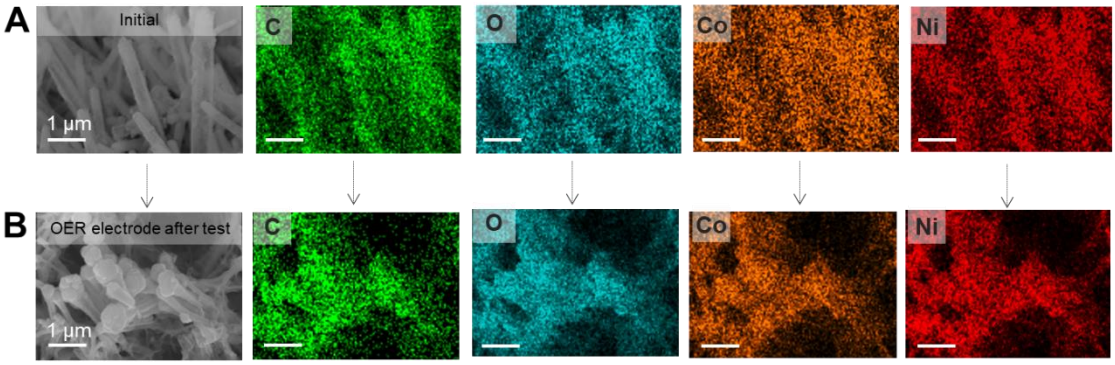

Figure S8. SEM-EDX mapping and elemental analysis of the Ni/Co/Co_3O_4@C (A) before and (B) after the OER.

Table S1. The elemental composition of the samples evaluated by SEM-EDX analysis.

Sample	Elemental composition			
	C [wt%]	**O** [wt%]	**Ni** [wt%]	**Co** [wt%]
Co-MOF	55.57	23.77	0	20.66
Ni-MOF	46.35	28.13	25.52	0
Co/Ni-MOF	36.95	22.52	19.14	21.39
Co/Co_3O_4@C	45.68	9.48	0	44.84
Ni@C	54.84	4.67	40.49	0
Ni/Co/Co_3O_4@C	45.14	8.86	21.36	24.64

Table S2. Comparison of electrocatalytic performances of various bifunctional electrocatalysts.

Sample	OER overpotential		HER overpotential		Water splitting voltage	Durability	Ref.
	@ 30 mA/cm^2 [mV]	@ 100 mA/cm^2 [mV]	@ 30 mA/cm^2 [mV]	@ 100 mA/cm^2 [mV]	@ 20 mA/cm^2 [V]	[%@h]	
Ni/Co/Co_3O_4@C	246	350	143	224	1.6	91.6@24	This work
Ni_3Se_4	231	255	175	300	1.55	100@8	S3
FeNiP/P-G	245	291	200	225	1.63	100@20	S4
FeMn-MOF	265	364	215	330	1.57	90@12	S5
Co-S-Mo	295	322	230	290	1.72	88.2@25	S6
$FeNiSe_2$	270	333	425	240	1.64	70@6	S7
Co/Ni-MOF@Se	291	-	325	340	1.66	98@20	S8
NiCoP	270	346	120	175	1.56	94@11	S9
$FeNi_3$/$NiFeO_x$	270	-	175	-	1.66	75@2.5	S10
Ni-Co-P hollow	215	346	215	265	1.71	93.4@20	S11
CoFeP hollow	370	-	225	-	1.6	90@12	S12

Supporting references

[S1]. G. Greczynski and L. Hultman, Compromising science by ignorant instrument calibration-need to revisit half a century of published XPS data. *Angew. Chemie. Int. Ed.*, 2020, **59**, 5002–5006.

[S2]. S. D. Fang, F. He, J. Xie and L. Xue, Calibration of binding energy positions with C1s for XPS results. *J. Wuhan Univ. Technol. Mater. Sci. Ed.*, 2020, **35**, 711–718.

[S3]. S. Anantharaj, J. Kennedy and S. Kundu, Microwave-initiated facile formation of Ni_3Se_4 nanoassemblies for enhanced and stable water splitting in neutral and alkaline media. *ACS Appl. Mater. Interfaces.*, 2017, **9**, 8714–8728.

[S4]. F. Bu, W. Chen, M. F. Aly Aboud, I. Shakir, J. Gu and Y. Xu, Microwave-assisted ultrafast synthesis of adjustable bimetal phosphide/graphene heterostructures from MOFs for efficient electrochemical water splitting. *J. Mater. Chem. A.*, 2019, **7**, 14526–14535.

[S5]. H. Guan, N. Wang, X. Feng, S. Bian, W. Li and Y. Chen, FeMn bimetallic MOF directly

applicable as an efficient electrocatalyst for overall water splitting. *Colloids Surf. A Physicochem. Eng. Asp.*, 2021, **624**, 126596.

[S6]. S. Shit, W. Jang, S. Bolar, N. C. Murmu, H. Koo and T. Kuila, Effect of ion diffusion in cobalt molybdenum bimetallic sulfide toward electrocatalytic water splitting. *ACS Appl. Mater. Interfaces*, 2019, **11**, 21634–21644.

[S7]. K. C. Majhi and M. Yadav, Bimetallic chalcogenide nanocrystallites as efficient electrocatalyst for overall water splitting. *J. Alloys Compd.*, 2021, **852**, 156736.

[S8]. P. Luo, Z. Pang, Z. Qin, T. Wei, S. Li, Y. Hu and C. Wei, Strategies for improving Co/Ni-based bimetal-organic framework to water splitting. *Int. J. Hydrogen Energy*, 2020, **45**, 28240–28251.

[S9]. C. Du, L. Yang, F. Yang, G. Cheng and W. Luo, Nest-like NiCoP for highly efficient overall water splitting. *ACS Catal.*, 2017, **7**, 4131–4137.

[S10]. X. Yan, L. Tian, K. Li, S. Atkins, H. Zhao, J. Murowchick, L. Liu and X. Chen, $FeNi_3/NiFeO_x$ nanohybrids as highly efficient bifunctional electrocatalysts for overall water splitting. *Adv. Mater. Interfaces*, 2016, **3**, 1600368.

[S11]. [S11] E. Hu, Y. Feng, J. Nai, D. Zhao, Y. Hu and X. W. Lou, Construction of hierarchical Ni–Co–P hollow nanobricks with oriented nanosheets for efficient overall water splitting. *Energy Environ. Sci.*, 2018, **11**, 872–880.

[S12]. Y. Du, H. Qu, Y. Liu, Y. Han, L. Wang and B. Dong, Bimetallic CoFeP hollow microspheres as highly efficient bifunctional electrocatalysts for overall water splitting in alkaline media. *Appl. Surf. Sci.*, 2019, **465**, 816–823.